Refinement of the Crystal Structure of Pr₇O₁₂ by Powder Neutron Diffraction*

By R. B. Von Dreele† and L. Eyring

Department of Chemistry, Arizona State University, Tempe, Arizona 85281, U.S.A.

and A. L. Bowman and J. L. Yarnell

Los Alamos Scientific Laboratory, University of California, Los Alamos, New Mexico 87544, U.S.A.

The structure of the intermediate phase Pr_7O_{12} was determined by powder neutron diffraction. The atomic parameters were refined by least-squares fitting of the diffraction profile. Pr_7O_{12} crystallizes in the space group $R\bar{3}$ with $a = 6\cdot7431$ (6) Å, $\alpha = 99\cdot306$ (6)° and $Z = 1$. The standard profile residual was $0\cdot129$ for a data: parameter ratio of 707:20. Pr_7O_{12} is derived from the MO_2 fluorite structure and has a pair of vacancies in the oxygen array situated along the rhombohedral [111] axis. Both the anion and cation arrays relax around the vacancies to form M_4O_5 defect clusters which occur in pairs with one metal atom in common.

Introduction

The rhombohedral intermediate phase, R_7O_{12}, which dominates the phase diagram of the higher oxides of the rare earths, was first observed in the praseodymium system (Ferguson, Guth & Eyring, 1954) and was subsequently characterized in the TbO_x-O_2 system (Baenziger, Eick, Schuldt & Eyring, 1961) and the CeO_x-O_2 system (Bevan, 1955; Bevan & Kordis, 1964). The importance of this phase among those of the oxygen-deficient fluorite-related systems was more fully appreciated when it was found to occur in the ternary systems W–Y–O (Borchardt, 1963), W–R–O for R = Tb–Lu (McCarthy, Fischer, Johnson & Gooden, 1972), U–R–O for R = Y, Lu (Bartram, 1966) and Zr–Sc–O (Thornber, Bevan & Graham, 1968). The complete structure was determined for two of these ternary phases, UY_6O_{12} (Bartram, 1966) and $Zr_3Sc_4O_{12}$ (Thornber, Bevan & Graham, 1968).

Because of the key importance of the R_7O_{12} phase in the homologous series (R_nO_{2n-2}) of binary rare-earth oxides considerable effort has been made to determine accurately its crystal structure. It has not been possible to obtain suitable untwinned single crystals for X-ray analysis; therefore a structure analysis technique has been employed which obviates this requirement.

Recent advances in the analysis of neutron powder diffraction data have permitted the investigation of some quite complex structures. Rietveld (1967, 1969) has shown that the entire profile of a powder diffraction pattern can be fitted by a least-squares refinement of the structure parameters. By using high-resolution neutron powder diffraction data, Von Dreele & Cheetham (1974) have examined a Ti–Nb oxide with 56 variable parameters from a diffraction profile composed of over 800 unique Bragg reflections. For the rare-earth oxides neutron diffraction provides a very sensitive probe of the anion array because of the relatively great scattering power of oxygen. Indeed, the scattering factor of oxygen, $0\cdot577 \times 10^{-14}$ m, is greater than that of praseodymium, $0\cdot44 \times 10^{-14}$ m (Neutron Diffraction Commission, 1969). This is of considerable importance because it is the anion array which provides the major structural difference between the intermediate rare-earth oxide phases.

Structure determination

A fine, well crystallized powder sample of Pr_7O_{12} was prepared by heating the oxide (99·999% Pr, Trona Chemical Co.) at 780 °C in a controlled oxygen atmosphere of 10 torr for one week followed by rapid cooling. An X-ray powder diffraction pattern of the sample thus obtained was identical with that of well characterized Pr_7O_{12} (Sawyer, Hyde & Eyring, 1965).

Powder neutron diffraction data for Pr_7O_{12} were collected at room temperature on a modified triple-axis diffractometer at the Omega West Reactor, Los Alamos Scientific Laboratory. A mean neutron wavelength of 1·27963 (8) Å was obtained by reflection from the (220) planes of a Cu monochromator at a $2\theta_m$ of 60°. The flux at the sample was $\sim 10^5$ n cm^{-2} s^{-1}. The wavelength was calculated from the diffraction pattern of a NbO standard; these diffraction peaks were accurately Gaussian in shape. The Pr_7O_{12} sample was contained in a sealed silica tube (1·5 cm diameter and 5·0 cm long) under vacuum. The data were collected in two identical scans over the range $10\cdot0 \le 2\theta \le 90\cdot0°$ in steps of $0\cdot10° \ 2\theta$. The counting time at each step was determined by the time required for an incident beam monitor count of 100 K obtained with a fission counter. The two scans showed no systematic differences and were therefore summed point by point to give the data set used in the least-squares analysis. The resulting

profile contained 707 observations with some contribution from the 280 unique accessible Bragg reflections. Absorption and extinction effects proved to be negligible and no corrections were necessary. The background corrections were obtained by linear interpolation between 19 values estimated at relatively clear portions of the diffraction profile and from a pattern taken of an empty silica sample tube.

The structural and lattice parameters for Pr_7O_{12} were refined by full-matrix least-squares fitting of the powder diffraction profile.* In this method, each Bragg reflection is assumed to be Gaussian in shape and the profile is calculated from the sum of the Gaussian peaks corresponding to the set of reflections. Thus, each intensity observation (Y_{obs}) is the sum of contributions from the peaks which overlap at that point and the weighted difference between the observed and calculated profiles is minimized by a least-squares refinement. Several profile parameters, *i.e.* lattice parameters, diffractometer zero-point (Z), and three half-width parameters (U, V, W) from the function (Caglioti, Paoletti & Ricci, 1958)

$$(H_K)^2 = U \tan^2 \theta_K + V \tan \theta_K + W$$

are refined simultaneously with the atomic positional and thermal parameters.

The starting values of the profile parameters (U, V, W, Z) were obtained from the diffraction pattern of the NbO standard. The lattice parameters were taken from the Guinier X-ray powder pattern analysis of Sawyer, Hyde & Eyring (1965) which gave $a = 6\cdot741$ (3) Å and $\alpha = 99\cdot28°$ for the rhombohedral cell. The space group was taken as $R\bar{3}$, the same as found for UY_6O_{12} and ULu_6O_{12} (Bartram, 1966) which are isomorphous with Pr_7O_{12}. The initial coordinates were taken from the ideal fluorite positions in the rhombohedral cell (Table 1). Neutron scattering lengths of $0\cdot577 \times 10^{-14}$ m for oxygen and $0\cdot44 \times 10^{-14}$ m for praseodymium (Neutron Diffraction Commission, 1969) were used in the refinements. Each observation was assigned a weight, $w = 250/I$, where I is the total count including the background (Rietveld, 1969; Hewat, 1973a). The least-squares analysis proceeded smoothly and gave a profile residual $R_p = \sum |Y_{obs} - Y_{calc}|/\sum |Y_{obs}|$ and a weighted residual $R_{pw} = [\sum w(Y_{obs} -$

* A modified version of a Fortran program written by H. M. Rietveld was used in this analysis.

$Y_{calc})^2/\sum w(Y_{obs})^2]^{1/2}$ of $0\cdot129$ and $0\cdot127$, respectively, for a data: parameter ratio of 707:20.* The observed and calculated profile intensities from the final refinement are shown in Fig. 1. The lattice parameters obtained in this refinement are identical to those obtained from the X-ray study with $a = 6\cdot7431$ (6) Å and $\alpha = 99\cdot306$ (6)°. The refined atomic coordinates and thermal parameters for Pr_7O_{12} are given in Table 1 along with the corresponding ideal coordinates from the fluorite structure.

Discussion

The structure of Pr_7O_{12} is in agreement with that originally suggested for Tb_7O_{12} by Baenziger *et al.* (1961) and that found for UY_6O_{12} (Bartram, 1966) and $Zr_3Sc_4O_{12}$ (Thornber *et al.*, 1968). The rhombohedral cell is derived from a cubic fluorite sublattice and is

* In this analysis it is assumed that the profile observations are independent and that only the diagonal terms of the weight matrix (Hamilton, 1964) used in the least-squares are nonzero. This is justified because *experimentally* the intensity observed at a particular profile point is not affected by errors in the intensities of neighboring profile points. In the few cases where both a powder diffraction profile analysis and a high-precision single-crystal analysis have been performed, the differences between the results are in satisfactory agreement with the estimated standard deviations obtained from the powder experiment (Hewat, 1973b).
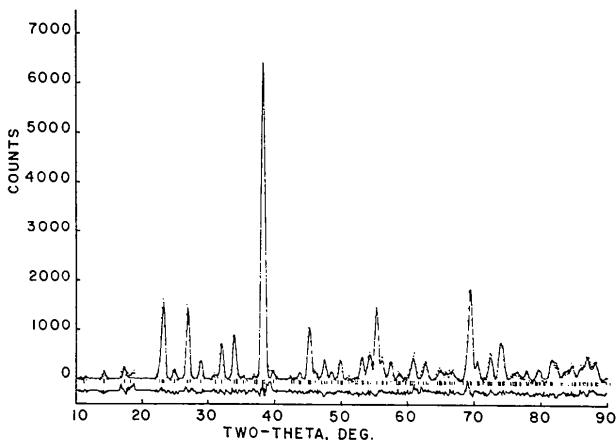

Fig. 1. The observed and calculated diffraction profiles for Pr_7O_{12} (observed profile: dotted curve; calculated profile: full curve). The difference profile and reflection positions are also shown.

Table 1. *Fractional atomic coordinates* ($\times 10^4$) *and thermal parameters for* Pr_7O_{12}

Figures in parentheses are estimated standard deviations obtained from least-squares analysis.

	Actual coordinates				Fluorite coordinates		
	x	y	z	B_{iso}	x	y	z
Pr(1)	0	0	0	0·59 (8)*	0	0	0
Pr(2)	3005 (12)	1405 (11)	6018 (10)	0·59 (8)*	2857	1429	5714
O(1)	9338 (13)	654 (10)	6860 (11)	1·10 (5)*	9643	1071	6786
O(2)	5684 (13)	4125 (11)	8230 (10)	1·10 (5)*	5357	3929	8214
Vacancy	2500	2500	2500	–	2500	2500	2500

* Parameters not refined independently.

oriented such that the trigonal axis coincides with one of the cubic $\langle 111 \rangle$ axes. This cell has a volume $\frac{7}{4}$ times the fluorite cell and has a pair of vacancies (V) in the oxygen array situated along the rhombohedral [111] to give the cell content Pr_7O_{12}.

The spatial relationship of the vacancies in the planes perpendicular to the [111] axis can be seen in Fig. 2. These slabs, which consist of a plane of metal atoms and the two neighboring planes of oxygen atoms, stack in a pseudocubic fashion $(-ABCABC-)$ such that a vacancy is placed above and below the metal position with trigonal symmetry [Pr(1)]. As a result, in each rhombohedral cell one metal atom [Pr(1)] is six-coordinate and six metal atoms [Pr(2)] are seven-coordinate.

The coordination geometry around Pr(1) can be considered either as a trigonally compressed octahedron or else derived from a cube with empty anion sites at opposite vertices. The O–M–O angles (Table 2) of $101 \cdot 0°$ in the trigonal face and $79 \cdot 0°$ between the faces are almost exactly half-way between the values expected for a cube, $109 \cdot 5°$ and $70 \cdot 5°$ and an octahedron, $90°$ for both. A very similar coordination was found in both $Zr_3Sc_4O_{12}$ and $Zr_{10}Sc_4O_{26}$ (Thornber *et al.*, 1968) in which the O–M–O angles are almost identical to those obtained in this analysis. In UY_6O_{12} this site is more closely octahedral and the corresponding O–M–O angles are $94 \cdot 8°$ and $85 \cdot 2°$ respectively. This difference may result from the much shorter U–O bond, $2 \cdot 07$ Å, requiring a more nearly close-packed oxygen array around the metal atom than either the Pr(1)–O bond, $2 \cdot 22$ Å, or the (Zr,Sc)–O bond, $2 \cdot 16$ Å. A comparison of predicted Pr–O bond lengths from ionic radii
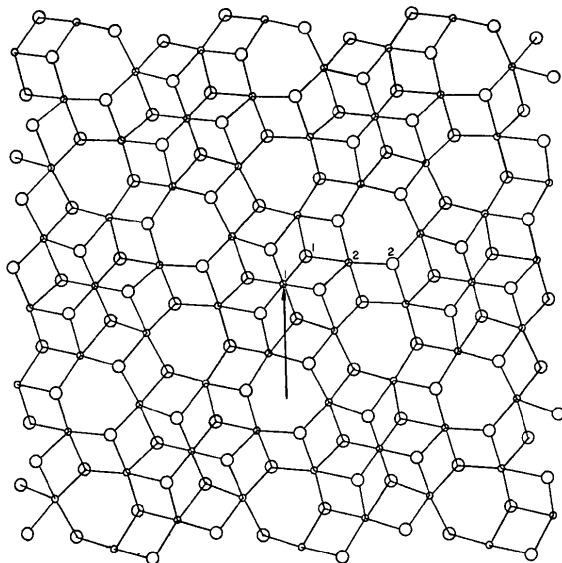

Fig. 2. Section of the Pr_7O_{12} structure perpendicular to the [111] axis. A plane of metal atoms and the two neighboring planes of oxygen atoms are shown. The large circles are oxygen atoms and the small circles are praseodymium atoms. The stacking vector is also shown.

Table 2. *Selected interatomic distances* (Å) *and angles in* Pr_7O_{12}

Figures in parentheses are estimated standard deviations.

(a) Intra-cluster distances and angles

V^*—O(1)	2·421 (7)	O(1)–V—O(1)	90·2 (2)
V—O(2)	2·565 (8)	O(1)–V—O(2)	90·2 (2)
V—Pr(1)	2·402 (1)	O(1)–V—O(2')	87·7 (3)
V—Pr(2)	2·584 (7)	O(2)–V—O(2')	92·0 (2)
Pr(1)–O(1)	2·222 (7)	Pr(1)–V—Pr(2)	111·3 (1)
Pr(2)–O(1)	2·370 (9)	Pr(2)–V—Pr(2')	107·6 (2)
Pr(2)–O(2)	2·263 (12)	O(1)–Pr(1)–O(1)	101·0 (2)
Pr(2)–O(2')	2·404 (12)	O(1)–Pr(2)–O(2)	96·4 (4)
O(1)–O(1)	3·430 (11)	O(1)–Pr(2)–O(2')	95·4 (4)
O(1)–O(2)	3·532 (11)	O(2)–Pr(2)–O(2')	104·4 (5)
O(1)–O(2')	3·455 (11)	O(1)–Pr(1)–O(1')	79·0 (2)
O(2)–O(2')	3·689 (11)		

(b) Inter-cluster distances and angles

Pr(2)–O(1')	2·368 (10)	V—Pr(2)–O(1')	172·4 (4)
Pr(2)–O(1'')	2·615 (12)	O(1'')–Pr(2)–O(2')	164·6 (4)
Pr(2)–O(2'')	2·372 (11)	O(2'')–Pr(2)–O(2)	172·3 (4)
Pr(2)–O(2''')	2·455 (9)	O(2''')–Pr(2)–O(1)	163·0 (4)
O(1)–O(1'')	2·852 (16)	O(1)—Pr(2)–O(1'')	69·6 (4)
O(1)–O(2'')	2·941 (11)	O(1)—Pr(2)–O(2'')	76·7 (3)
O(1')–O(1'')	2·826 (10)	O(1')—Pr(2)–O(1'')	68·9 (4)
O(1')–O(2'')	2·967 (11)	O(1')—Pr(2)–O(2'')	77·5 (4)
O(1')–O(2''')	2·941 (11)	O(1')—Pr(2)–O(2''')	75·1 (3)
O(1'')–O(2)	2·967 (11)	O(1'')—Pr(2)–O(2)	74·5 (3)
O(2)–O(2''')	2·885 (10)	O(2)—Pr(2)–O(2''')	75·3 (3)
O(2')–O(2'')	2·845 (15)	O(2')—Pr(2)–O(2'')	73·1 (4)
O(2')–O(2''')	2·885 (10)	O(2')—Pr(2)–O(2''')	72·9 (3)

* Vacancy (V) position assumed to be at $x = 0·25$, $y = 0·25$, $z = 0·25$.

(Shannon & Prewitt, 1969) gives a value of $2 \cdot 16$ Å for Pr^{IV} and $2 \cdot 39$ Å for Pr^{III} in octahedral coordination. In addition, the Pr^{IV}–O bond lengths in the perovskite, $BaPrO_3$, are $2 \cdot 22$ and $2 \cdot 23$ Å (Jacobson, Tofield & Fender, 1972), therefore the Pr(1) site probably contains mostly tetravalent praseodymium. The U^{VI} in UY_6O_{12} was also found in this six-coordinate site but no evidence for cation ordering was observed in $Zr_3Sc_4O_{12}$. Since the ionic radii of Zr^{IV} and Sc^{III} are virtually identical it would appear that cation ordering in the M_7O_{12} structures depends on size rather than ionic charge with the smaller ion preferring the six-coordinate site.

The anions surrounding the seven-coordinate metal atom can best be described as being at the vertices of a very distorted cube having one open site. This can be appreciated from the Pr(2)–O distances where the shortest is $2 \cdot 26$ Å, the longest is $2 \cdot 61$ Å and the five others range from $2 \cdot 37$ to $2 \cdot 45$ Å. It is interesting that the latter are nearly the same length as calculated from ionic radii for Pr^{III}–O in an octahedron, $2 \cdot 39$ Å and for Pr^{IV}–O in a cube, $2 \cdot 37$ Å (Shannon & Prewitt, 1969). If Pr(1) is tetravalent then the six Pr(2) atoms may be considered as a random mixture of four Pr^{III} atoms and two Pr^{IV} atoms. By comparison, the Pr–O distance in PrO_2 based on the lattice parameter of Sieglaff & Eyring (1957) is $2 \cdot 37$ Å for cubic coordination and in Pr_2O_3 (bixbyite) the Pr–O distances fall in

the range 2·33 to 2·46 Å for six-coordination (Eyring & Baenziger, 1962). The range of O–Pr(2)–O angles, 68·9 to 77·5°, also shows the distortions from cubic geometry.

The source of these distortions can be ascribed principally to a relaxation of the cation and anion arrays around the vacancy position to form an M_4O_6 defect cluster. If one assumes the vacancy (V) to be positioned at the ideal fluorite site ($\frac{1}{4}\frac{1}{4}\frac{1}{4}$) in the rhombohedral cell, then the V–O(1) and V–O(2) distances are 2·42 and 2·56 Å, respectively. If there had been no distortions then the V–O distances would be the same as the O–O distance, 2·73 Å, in PrO_2. Despite these large shifts, there is little angular distortion since the anion coordination about the vacancy remains octahedral; all the O–V–O angles are nearly 90°. There is a similar relaxation of the cation array about the vacancy; the V–Pr(1) and V–Pr(2) distances, 2·40 and 2·58 Å respectively, are much longer than the Pr–O distance, 2·33 Å, in PrO_2. Again, the angular distortion is slight since the Pr–V–Pr angles are virtually unchanged from the tetrahedral Pr–O–Pr angle, 109·5°, found in PrO_2. In $Zr_3Sc_4O_{12}$ a much greater relaxation of the oxygen array occurs; the oxygen atoms are displaced toward the vacancy position by ca 0·50 Å. However, no distortion of the metal atom array was noted. Steele & Fender (1974) also found a much larger relaxation of the anion array for the defect fluorite structures in the ZrO_2:Y_2O_3 and ZrO_2:Yb_2O_3 solid solutions. The shifts correspond to a V–O distance of 2·16 Å compared with the average value of 2·49 Å for Pr_7O_{12}. They also found that the corresponding ThO_2:Y_2O_3 and CeO_2:Y_2O_3 solid solutions show no displacement of the near-neighbor oxygen atoms towards a vacancy. It was apparent that the amount of displacements is related to the cation ionic radius, the small Zr^{4+} ion allowing a much greater shift than the large Th^{4+} ion. In Pr_7O_{12} the anion displacements are much less than in $Zr(Y)O_{2-x}$ and $Zr_3Sc_4O_{12}$ as appropriate for the larger cation; the M–O distances in the M_4O_6 defect cluster are 2·24 Å for $Zr(Y)O_{2-x}$ and 2·09 Å (average) for $Zr_3Sc_4O_{12}$ but are 2·31 Å (average) for Pr_7O_{12}.

These M_4O_6 clusters then comprise the entire structure of Pr_7O_{12}. Two clusters share a metal atom [Pr(1)] in common and this pair of clusters has the composition M_7O_{12}. These cluster pairs then pack so that the

other metal atoms [Pr(2)] are seven-coordinate. Since there are no regions of eight-coordinate metal atoms in this structure it is difficult to assess the importance of either the individual M_4O_6 clusters or the M_7O_{12} cluster pairs in the structures of the higher praseodymium oxides, and this analysis must await a more detailed examination of these other phases.

References

BAENZIGER, N. C., EICK, H. A., SCHULDT, H. S. & EYRING, L. (1961). J. Amer. Chem. Soc. 83, 2219–2223.
BARTRAM, S. F. (1966). Inorg. Chem. 5, 749–754.
BEVAN, D. J. M. (1955). J. Inorg. Nucl. Chem. 1, 49–59.
BEVAN, D. J. M. & KORDIS, J. (1964). J. Inorg. Nucl. Chem 26, 1509–1523.
BORCHARDT, H. J. (1963). Inorg. Chem. 2, 170–173.
CAGLIOTI, G., PAOLETTI, A. & RICCI, F. P. (1958). Nucl. Instrum. 3, 223–228.
EYRING, L. & BAENZIGER, N. C. (1962). J. Appl. Phys. 33, 428–433.
FERGUSON, R. E., GUTH, E. D. & EYRING, L. (1954). J. Amer. Chem. Soc. 76, 3890–3894.
HAMILTON, W. C. (1964). Statistics in Physical Science, pp. 146–149. New York: Ronlad Press.
HEWAT, A. W. (1973a). UKAEA Research Group Report RRL 73/239.
HEWAT, A. W. (1973b). J. Phys. C, Solid State Phys. 6, 2559–2572.
JACOBSON, A. J., TOFIELD, B. C. & FENDER, B. E. F. (1972). Acta Cryst. B28, 956–961.
McCARTHY, G. J., FISCHER, R. D., JOHNSON, G. G. JR & GOODEN, C. E. (1972). NBS Special Publication 364. Solid State Chemistry, pp. 397–411.
NEUTRON DIFFRACTION COMMISSION (1969). Acta Cryst. A25, 391–392.
RIETVELD, H. M. (1967). Acta Cryst. 22, 151–152.
RIETVELD, H. M. (1969). J. Appl. Cryst. 2, 65–71.
SAWYER, J. O., HYDE, B. G. & EYRING, L. (1965). Bull. Soc. Chim. Fr. pp. 1190–1199.
SHANNON, R. D. & PREWITT, C. T. (1969). Acta Cryst. B25, 925–946.
SIEGLAFF, C. L. & EYRING, L. (1957). J. Amer. Chem. Soc. 76, 5872–5874.
STEELE, D. & FENDER, B. E. F. (1974). J. Phys. C, Solid State Phys. 7, 1–11.
THORNBER, M. R., BEVAN, D. J. M. & GRAHAM, J. (1968). Acta Cryst. B24, 1183–1190.
VON DREELE, R. B. & CHEETHAM, A. K. (1974). Proc. Roy. Soc. 338, 311–326.